Triplet-triplet energy-transfer coupling: Theory and calculation

Zhi-Qiang You, Chao-Ping Hsu, and Graham R. Fleming

Citation: The Journal of Chemical Physics **124**, 044506 (2006); doi: 10.1063/1.2155433
View online: http://dx.doi.org/10.1063/1.2155433
View Table of Contents: http://scitation.aip.org/content/aip/journal/jcp/124/4?ver=pdfcov
Published by the AIP Publishing

Triplet-triplet energy-transfer coupling: Theory and calculation

Zhi-Qiang You
Institute of Chemistry, Academia Sinica, 128 Academia Road Section 2, Nankang, Taipei 115, Taiwan

Chao-Ping Hsu[a)]
Institute of Chemistry, Academia Sinica, 128 Academia Road Section 2, Nankang, Taipei 115, Taiwan and Institute of Molecular Sciences, National Chiao-Tung University, 1001 Ta Hsue Road, Hsinchu 300, Taiwan

Graham R. Fleming
Department of Chemistry, University of California, Berkeley, California 94720 and Lawrence Berkeley National Laboratory, Physical Biosciences Division, Berkeley, California 94720

(Received 3 October 2005; accepted 22 November 2005; published online 25 January 2006)

Triplet-triplet (TT) energy transfer requires two molecular fragments to exchange electrons that carry different spin and energy. In this paper, we analyze and report values of the electronic coupling strengths for TT energy transfer. Two different methods were proposed and tested: (1) Directly calculating the off-diagonal Hamiltonian matrix element. This direct coupling scheme was generalized from the one used for electron transfer coupling, where two spin-localized unrestricted Hartree-Fock wave functions are used as the zero-order reactant and product states, and the off-diagonal Hamiltonian matrix elements are calculated directly. (2) From energy gaps derived from configuration-interaction-singles (CIS) scheme. Both methods yielded very similar results for the systems tested. For TT coupling between a pair of face-to-face ethylene molecules, the exponential attenuation factor is 2.59 Å^{-1}(CIS/6-311+G**), which is about twice as large as typical values for electron transfer. With a series of fully stacked polyene pairs, we found that the TT coupling magnitudes and attenuation rates are very similar irrespective of their molecular size. If the polyenes were partially stacked, TT couplings were much reduced, and they decay more rapidly with distance than those of full-stacked systems. Our results showed that the TT coupling arises mainly from the region of close contact between the donor and acceptor frontier orbitals, and the exponential decay of the coupling with separation depends on the details of the molecular contacts. With our calculated results, nanosecond or picosecond time scales for TT energy-transfer rates are possible. © *2006 American Institute of Physics*. [DOI: 10.1063/1.2155433]

I. INTRODUCTION

Triplet-triplet (TT) energy transfer is a process of exchanging both spin and energy between a pair of molecules or molecular fragments. It plays an important role in many photophysical processes in chemistry[1–4] and biology.[5–7] When a closed-shell molecule is photoexcited to its singlet excited state, it may undergo intersystem crossing (ISC) to reach a triplet state. TT energy transfer may subsequently occur, and this provides a chance to design materials with interesting properties for potentially useful applications (see, for example, Refs. 2–4 and 8). In photosynthetic organisms, photoexcitation of chrolophylls (Chls) or bacteriochlorophylls (Bchls) under sunlight inevitably leads to the formation of triplet Chls or Bchls. For the sake of definiteness we focus only on Bchl:

$$\text{Bchl} \xrightarrow{h\nu} {}^1\text{Bchl}^* \xrightarrow{\text{ISC}} {}^3\text{Bchl}^*. \tag{1}$$

Through spin exchange (SE), reactive singlet oxygen is generated:

$$ {}^3\text{Bchl}^* + {}^3\text{O}_2 \xrightarrow{\text{SE}} \text{Bchl} + {}^1\text{O}_2^* \rightarrow \text{oxidative damages}. \tag{2}$$

Carotenoids (Cars) in photosynthetic proteins can directly quench triplet Bchls through a TT spin-exchange process, and thereby avoid the formation of reactive singlet oxygen:[9]

$$ {}^3\text{Bchl}^* + {}^1\text{Car} \xrightarrow{\text{SE}} {}^1\text{Bchl} + {}^3\text{Car}, \tag{3}$$

or can quench singlet oxygen directly:[10]

$$ {}^1\text{O}_2^* + {}^1\text{Car} \xrightarrow{\text{SE}} {}^3\text{O}_2 + {}^3\text{Car}. \tag{4}$$

The TT energy-transfer process can be viewed as two simultaneous electron transfers with different spin ($\alpha \rightarrow \alpha, \beta \rightarrow \beta$)(Fig. 1). It is similar to the Dexter exchange coupling in the singlet-singlet energy transfer,[11] which arises from exchanging electrons of the same spin but different energies. Therefore, in addition to the intrinsic importance of understanding the TT energy transfer, an understanding of the coupling mechanism should provide insight into Dexter exchange coupling.

In the singlet-singlet energy transfer, where the spin state of each fragment is conserved, it can be shown that the electronic coupling arises from:[11–15] (1) Coulombic coupling,

[a)]Author to whom correspondence should be addressed. Electronic mail:cherri@sinica.edu.tw

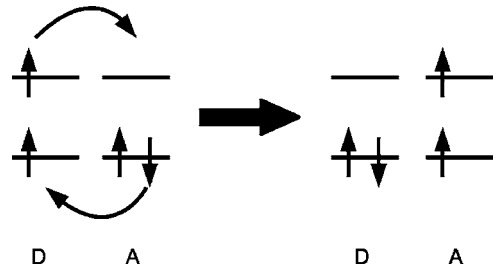

FIG. 1. A schematic picture of TT energy transfer as two simultaneous electron transfers between the donor (D) and acceptor (A).

which is the Coulomb interaction between electronic transitions. Under the dipole approximation, this interaction reduces to the well-known Förster dipole-dipole coupling; (2) Dexter exchange coupling, arising from the exchange integrals that account for the indistinguishability of the electrons in many-electron wave functions.[11] The Dexter coupling exists only at short donor-acceptor distance, since the exchange integrals are expected to decrease steeply with separation. At short distances, or for dipole-forbidden transitions, the dipole approximation breaks down, and the full Coulombic coupling may not follow a typical R^{-6} dipole-dipole form. Higher-order multipole interactions may lead to R^{-8} or steeper distance dependence. Moreover, if the close-contact geometry does not allow spherical harmonic expansion, there is no simple polynomial distance dependence.[16,17] Therefore, observation of a distance dependence that is steeper than R^{-6} is not sufficient to conclude that the Dexter exchange coupling is the relevant mechanism (see, for example, Refs. 18 and 19). To help resolve the difficulty of deducing the origin of electronic coupling from the experimental data, it is important to find reliable theoretical estimates of the magnitude of the Dexter coupling strength. Estimating magnitude of the TT coupling, a similar quantity, could shed light on this issue.

Experimental studies have shown that the TT exchange process behaves like two simultaneous electron transfers (ETs).[20,21] Recent findings using phenylene oligomers as spacers further support this picture. TT energy-transfer rates between Ru and Os dinuclear metal complexes were reported to decrease with separation exponentially by 0.32, 0.44, and 0.50 $Å^{-1}$,[2,3] while optically induced intervalence ET between Ru complexes had exponents of 0.084 or 0.118 $Å^{-1}$ (Ref. 22) for the *electronic couplings*. If the latter values are multiplied by a factor of 2 to convert to ET *rates*, the exponents for the ET are roughly half of those for the TT energy transfer.

Despite the fundamental importance of TT energy transfer in photophysics, theoretical characterization of TT coupling has been rather rare. In the 1960s, Jortner and coworkers studied the effect of exchange coupling on charge mobility in organic molecular crystals.[23–25] Using hydrogenlike orbitals, Levy and Speiser calculated the exchange integrals in covalently linked α-diketones and a number of aromatic fragments.[26] In Ref. 27, the TT exchange coupling between the two radical methylene groups of 1,4-dimethylenecyclohexane was estimated to demonstrate the relationship of TT energy transfer with electron and hole transfers. The Dexter exchange coupling was estimated to be of the order of 10^{-4} eV between a Bchl and a neurosporene in a number of arrangements.[28] Calculations using the Praiser-Parr-Pople (PPP) Hamiltonian yielded values on the order of 10^{-5} eV for the TT coupling between Bchls and lycopenes in the bacterial LH2 light-harvesting complex.[29] Such coupling strengths lead to transfer rates that are much smaller than those observed experimentally, which are on the nanosecond time scale.[8–10] A serious underestimate of the Coulomb coupling from the forbidden S_1 state of carotenoid is found in Refs. 28 and 29, possibly due to deficiencies in the semiempirically parametrized Hamiltonians.[17] Therefore, it is important to establish an *ab initio* based methodology to determine whether the mechanism or calculation method is responsible for the underestimates of exchange couplings.

Recent calculations employing the quantum Monte Carlo (QMC) approach have obtained a singlet-triplet energy gap within experimental errors (0.01 eV) for a porphyrin.[30] Such energy gaps result from the exchange integrals, and therefore provide a route to both TT and Dexter coupling magnitudes. No QMC estimate for TT coupling is yet available, and it is desirable to derive TT coupling values from wave-function-based models for future comparison.

ET coupling has been calculated via quantum chemistry methods, either by using a resonant condition at the transition state, and taking half of the energy gap between the lowest two adiabatic states as the coupling strength,[31] or by directly calculating the coupling matrix element term by term using unrestricted Hartree-Fock (UHF) charge-localized solutions.[32–34] In this work we explore whether the methods used for ET coupling can be generalized to calculate TT coupling. In particular, we discuss the theoretical grounds for using the direct coupling (DC) scheme and the energy-gap-based method to obtain TT energy-transfer coupling. Results for both symmetric and asymmetric small test systems will also be discussed.

II. THEORY AND METHODS

A. Direct coupling

The DC scheme is described in Refs. 32–35 for ET systems. It has also been used to estimate TT coupling for cyclohexane-spaced methylene radicals.[32] In this section we discuss the theoretical background of this coupling scheme.

To calculate the off-diagonal Hamiltonian matrix element, we need two zero-order wave functions that can properly represent the reactant and product states ("diabatic states" in the ET literature).[36] In the ET systems, it has been shown that UHF solutions can often provide good approximation for such charge-localized states. We propose that a similar scheme can be used for TT coupling. Namely, Ψ_r, the reactant state, is modeled by an UHF solution such that the donor fragment is in its triplet state, while the acceptor is in singlet state, and vice versa for Ψ_p, the product state.

To evaluate the transfer coupling between spin-localized states, we have

$$T_{rp} = \frac{H_{rp} - S_{rp}(H_{rr} + H_{pp})/2}{1 - S_{rp}^2}, \tag{5}$$

where

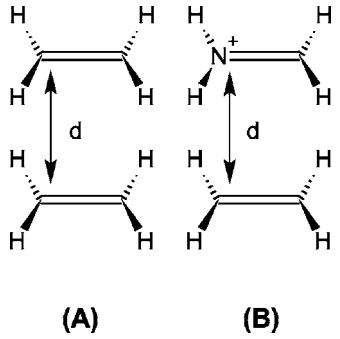

FIG. 2. Face-to-face arrangements of (A) two ethylenes, and (B) an ethylene and a methaniminium cation. d denotes the intermolecular distance.

$$H_{rp} = \langle \Psi_r | \hat{H} | \Psi_p \rangle = \int d\mathbf{x} \Psi_r^*(\mathbf{x}) \hat{H} \Psi_p(\mathbf{x}) \tag{6}$$

and

$$S_{rp} = \langle \Psi_r | \Psi_p \rangle = \int d\mathbf{x} \Psi_r^*(\mathbf{x}) \Psi_p(\mathbf{x}), \tag{7}$$

where $\mathbf{x}_i$ is the spin and spatial coordinates of electron i, H is the Hamiltonian for the system, and T_{rp} is the transfer integral, or transfer-matrix element defined in scattering problems, which is the effective full coupling. Ψ_r and Ψ_p are the spin-localized wave functions before and after energy transfer, respectively.

As an illustrative example, the TT coupling of a face-to-face arrangement of two ethylene molecules [Fig. 2(A)] is discussed. To simplify the problem, we assume that Ψ_r and Ψ_p are composed of the same set of core orbitals, and the differences are only in the four highest occupied spin-orbitals. Assuming that the reactant state is composed of one molecule (denoted as D) in its π-π^* triplet state while the other (denoted as A) is in its singlet ground state, (and vice versa for the the product state), we have

$$\Psi_r = |\Psi_{\text{core}} \pi_D \pi_D^* \pi_A \bar{\pi}_A|, \tag{8}$$

$$\Psi_p = |\Psi_{\text{core}} \pi_D \bar{\pi}_D \pi_A \pi_A^*|, \tag{9}$$

where $|\cdots|$ represents a Slater determinant, a short bar above an orbital ($\bar{\phi}$) denotes a β spin-orbital, while an orbital without the short bar (ϕ) is an α spin-orbital. The leading contribution in T_{rp} is[37]

$$\begin{aligned} T_{rp} \approx H_{rp} &= [\pi_D^* \bar{\pi}_A \| \bar{\pi}_D \pi_A^*] \\ &= [\pi_D^* \bar{\pi}_A | \bar{\pi}_D \pi_A^*] - [\pi_D^* \pi_A^* | \bar{\pi}_D \bar{\pi}_A] \\ &= -[\pi_D^* \pi_A^* | \bar{\pi}_D \bar{\pi}_A], \end{aligned} \tag{10}$$

where the two-electron integrals are defined as

$$[ij \| kl] \equiv [ij|kl] - [il|kj] \tag{11}$$

and

$$\begin{aligned} [ij|kl] &= [\chi_i \chi_j | \chi_k \chi_l] \\ &= \int d\mathbf{x}_1 d\mathbf{x}_2 \chi_i^*(\mathbf{x}_1) \chi_j(\mathbf{x}_1) \frac{1}{r_{12}} \chi_k^*(\mathbf{x}_2) \chi_l(\mathbf{x}_2). \end{aligned} \tag{12}$$

As shown in Eq. (10), the leading term in T_{rp} is an exchange integral, which gives rise to the "exchange" nature of the TT coupling, and is essentially the same as the Dexter coupling integral.[11]

In DC calculations, the expression in Eq. (5) is used. The effects of S_{rp}, as well as details in the different core orbitals, are fully accounted for. The spin-localized UHF solutions Ψ_r and Ψ_p were typically calculated using transition-state geometry [R=0.5 in Eq. (25) below for symmetric system, or at the minimun-energy gap for asymmetric systems] from initial solutions that are spin localized, which were obtained from a geometry composed of an optimized triplet and a singlet molecules. For jobs with asymmetric molecules, a quintet state was sometimes used as a starting point to find the spin-localized triplet state.

B. Energy-gap-based method: Configuration-interaction singles

In a two-state model, if the noninteracting states are degenerate, half of the eigenenergy difference is exactly the coupling between reactant and product states. We tested to see if a simple *ab initio* configuration-interaction-singles (CIS) scheme[38] can give reasonable results for exchange couplings.

We performed a CIS calculation with a singlet reference while solving for the lowest two triplet states. For two ethylenes separated at 4.5 Å, the first two triplet states obtained via CIS/6-31G* from the singlet ground state reference, in their M_s=1 configurations, are

$$\begin{aligned} \Psi_1^{\text{CIS}} = &- 0.6752 |\Psi_{\text{core}} \phi_1 \phi_2 \bar{\phi}_2 \phi_4| \\ &+ 0.7217 |\Psi_{\text{core}} \phi_1 \bar{\phi}_1 \phi_2 \phi_3| + \cdots, \end{aligned} \tag{13}$$

$$\begin{aligned} \Psi_2^{\text{CIS}} = &- 0.6558 |\Psi_{\text{core}} \phi_1 \phi_2 \bar{\phi}_2 \phi_3| \\ &+ 0.7019 |\Psi_{\text{core}} \phi_1 \bar{\phi}_1 \phi_2 \phi_4| + \cdots, \end{aligned} \tag{14}$$

where Ψ_{core} denotes a collection of core molecular orbitals. To gain insights from the two solutions, we assumed that the ideal solutions are composed of two equally populated single-excitation configurations, with other minor contributions ignored:

$$\begin{aligned} \Psi_1^{\text{CIS}} \approx &- (2)^{-1/2} |\Psi_{\text{core}} \phi_1 \phi_2 \bar{\phi}_2 \phi_4| \\ &+ (2)^{-1/2} |\Psi_{\text{core}} \phi_1 \bar{\phi}_1 \phi_2 \phi_3|, \end{aligned} \tag{15}$$

$$\begin{aligned} \Psi_2^{\text{CIS}} \approx &- (2)^{-1/2} |\Psi_{\text{core}} \phi_1 \phi_2 \bar{\phi}_2 \phi_3| \\ &+ (2)^{-1/2} |\Psi_{\text{core}} \phi_1 \bar{\phi}_1 \phi_2 \phi_4|. \end{aligned} \tag{16}$$

In the following, we further analyze the lowest two CIS triplet wave functions to see if they are linear combinations of spin-localized transitions.

In a symmetric arrangement, the molecular orbitals are delocalized. The lowest CIS excited states are excitations from the delocalized orbitals (denoted as ϕ below), mainly composed of the localized π orbitals and π^* orbitals:

$$\phi \approx \frac{1}{\sqrt{2 \pm 2s}}(\pi_D \pm \pi_A). \tag{17}$$

Here, $s = \int d\mathbf{x}\, \pi_D(\mathbf{x})\pi_A(\mathbf{x})$ is the overlap integral of the two localized orbitals. In order to keep only the major characteristics, the overlap integral s is ignored as a further simplification. The approximate compositions of the four delocalized orbitals involved in the two lowest CIS excited states are

$$\begin{aligned}
&\phi_1 \approx 2^{-1/2}(\pi_A - \pi_D), \quad \bar{\phi}_1 \approx 2^{-1/2}(\bar{\pi}_A - \bar{\pi}_D),\\
&\phi_2 \approx 2^{-1/2}(\pi_D + \pi_A), \quad \bar{\phi}_2 \approx 2^{-1/2}(\bar{\pi}_D + \bar{\pi}_A),\\
&\phi_3 \approx 2^{-1/2}(\pi_D^* - \pi_A^*), \quad \bar{\phi}_3 \approx 2^{-1/2}(\bar{\pi}_D^* - \bar{\pi}_A^*),\\
&\phi_4 \approx 2^{-1/2}(\pi_D^* + \pi_A^*), \quad \bar{\phi}_4 \approx 2^{-1/2}(\bar{\pi}_D^* + \bar{\pi}_A^*),
\end{aligned} \tag{18}$$

where D denotes one of the fragment named donor, and A is the other (acceptor). $\pi_{A/D}$ and $\pi^*_{A/D}$ are localized molecular orbitals involved in the TT energy-transfer process.

We next show that spin-localized states can be obtained from a linear combination of Ψ_1^{CIS} and Ψ_2^{CIS}:

$$\begin{aligned}
&\frac{1}{\sqrt{2}}(\Psi_1^{\mathrm{CIS}} + \Psi_2^{\mathrm{CIS}})\\
&\quad = \tfrac{1}{4}(-|\Psi_{\mathrm{core}}(\pi_A - \pi_D)(\pi_D + \pi_A)(\bar{\pi}_D + \bar{\pi}_A)\pi_D^*|\\
&\qquad + |\Psi_{\mathrm{core}}(\pi_A - \pi_D)(\bar{\pi}_A - \bar{\pi}_D)(\pi_D + \pi_A)\pi_D^*|)\\
&\quad = \tfrac{1}{2}|\Psi_{\mathrm{core}}(\pi_A - \pi_D)\bar{\pi}_A(\pi_D + \pi_A)\pi_D^*|\\
&\quad = |\Psi_{\mathrm{core}}\pi_D\pi_D^*\pi_A\bar{\pi}_A| \approx \Psi_r^{\mathrm{loc}},
\end{aligned} \tag{19}$$

which is a configuration with its spin localized in the donor fragments. We therefore assigned it as the reactant state. In the derivation of Eq. (19), standard operations for determinants were used (for example, see Ref. 39). Similarly, the other state from a linear combination of Ψ_1^{CIS} and Ψ_2^{CIS} is

$$\begin{aligned}
&\frac{1}{\sqrt{2}}(\Psi_1^{\mathrm{CIS}} - \Psi_2^{\mathrm{CIS}})\\
&\quad = \tfrac{1}{4}(|\Psi_{\mathrm{core}}(\pi_A - \pi_D)(\pi_D + \pi_A)(\bar{\pi}_D + \bar{\pi}_A)\pi_A^*|\\
&\qquad + |\Psi_{\mathrm{core}}(\pi_A - \pi_D)(\bar{\pi}_A - \bar{\pi}_D)(\pi_D + \pi_A)\pi_A^*|)\\
&\quad = |\Psi_{\mathrm{core}}\pi_D\bar{\pi}_D\pi_A\pi_A^*| \approx \Psi_p^{\mathrm{loc}}.
\end{aligned} \tag{20}$$

Therefore, the two CIS triplet states are mainly composed of two spin-localized states. To see if the energy gap derived from the two states gives rise to TT coupling, we have[37]

$$\begin{aligned}
E_1^{\mathrm{CIS}} &= \langle \Psi_1^{\mathrm{CIS}}|\hat{H}|\Psi_1^{\mathrm{CIS}}\rangle\\
&= \tfrac{1}{2}(E_{\mathrm{HF}} + \epsilon_2^- - \epsilon_3 - [\phi_3\phi_3 \| \bar{\phi}_2\bar{\phi}_2]\\
&\quad + E_{\mathrm{HF}} + \epsilon_1^- - \epsilon_4 - [\phi_4\phi_4 \| \bar{\phi}_1\bar{\phi}_1]\\
&\quad - 2[\phi_4\phi_3 \| \bar{\phi}_2\bar{\phi}_1]),
\end{aligned} \tag{21}$$

$$\begin{aligned}
E_2^{\mathrm{CIS}} &= \langle \Psi_2^{\mathrm{CIS}}|\hat{H}|\Psi_2^{\mathrm{CIS}}\rangle\\
&= \tfrac{1}{2}(E_{\mathrm{HF}} + \epsilon_1^- - \epsilon_3 - [\phi_3\phi_3 \| \bar{\phi}_1\bar{\phi}_1]\\
&\quad + E_{\mathrm{HF}} + \epsilon_2^- - \epsilon_4 - [\phi_4\phi_4 \| \bar{\phi}_2\bar{\phi}_2]\\
&\quad - 2[\phi_4\phi_3 \| \bar{\phi}_1\bar{\phi}_2]),
\end{aligned} \tag{22}$$

where ϵ_i is the molecular-orbital energy for ψ_i (i.e., an eigenvalue of the Fock matrix), and the two-electron integral $[\cdots\|\cdots]$ is as defined in Eq. (11). The energy splitting of two states in the molecular-orbital representation is therefore

$$\begin{aligned}
E_2^{\mathrm{CIS}} - E_1^{\mathrm{CIS}} &= \tfrac{1}{2}([\phi_3\phi_3|\bar{\phi}_2\bar{\phi}_2] - [\phi_3\phi_3|\bar{\phi}_1\bar{\phi}_1]\\
&\quad + [\phi_4\phi_4|\bar{\phi}_1\bar{\phi}_1] - [\phi_4\phi_4|\bar{\phi}_2\bar{\phi}_2]).
\end{aligned} \tag{23}$$

With Eq. (18), we convert the delocalized orbitals in Eq. (23) to the localized donor and acceptor molecular orbitals:

$$E_2^{\mathrm{CIS}} - E_1^{\mathrm{CIS}} = -2[\pi_D^*\pi_A^*|\bar{\pi}_D\bar{\pi}_A], \tag{24}$$

which is twice the coupling in Eq. (10), and again it is approximately an exchange integral, arising from the indistinguishability of electrons.

C. Computational details

A developmental version of the Q-CHEM quantum chemistry program package was used for all calculations presented in this work.[40] The direct coupling scheme was integrated with formulas previously reported.[35] The optimized geometry for singlet and triplet single molecules was calculated using density-functional theory (DFT)/B3LYP with DZP basis sets. For simple test systems composed of small molecules, an approximate reaction coordinate R is often used in the literature:[34]

$$Q_i(R) = (1 - R)Q_i^r + RQ_i^p, \quad 0 \leqslant R \leqslant 1, \tag{25}$$

where Q_i represents the ith nuclear coordinate, superscripts r and p refer to the reactant and product nuclear coordinates that are composed of optimized singlet and triplet molecules, respectively, and R is the reaction coordinate ($R=0$ for the reactant and $R=1$ for the product). In the present work, we simply used the Cartesian coordinates (x_i, y_i, z_i), with the symmetric center as the origin, for Q_i. For a symmetric system such as the one shown in Fig. 2(A), $R=0.5$ was used for an approximate transition state.

III. RESULTS AND DISCUSSION

A. Direct coupling

The TT electronic coupling between two face-to-face ethylenes (as depicted in Fig. 2) was calculated using Eq. (5). Results with different basis sets and as a function of intermolecular distance are shown in Fig. 3. Results from small basis sets show a deviation from a straight line in the semilog plot; this reflects the limitations of Gaussian basis functions. The couplings calculated from large, diffusive basis sets exhibit an exponential distance dependence, a characteristic property of TT electronic coupling arising from the exchange integral.[11,20]

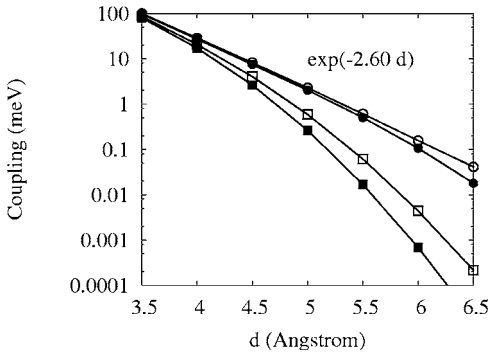

FIG. 3. Distance and basis set dependence of TT coupling, calculated from the DC scheme for the two-ethylene system. Bases sets used are as follows: 3-21G (filled squares), 6-31G* (open squares), DZP (filled circles), and 6-311+G* (open circles).

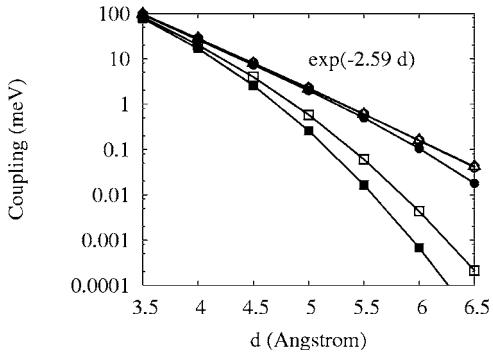

FIG. 4. Distance and basis set dependence of TT coupling. Shown are half of the CIS energy gaps between the two lowest triplet states for the two-ethylene system. Basis sets used are as follows: 3-21G (filled squares), 6-31G* (open squares), DZP (filled circles), 6-311+G* (open circles), and aug-cc-pVTZ (open triangles).

According to Eq. (10), the major term in the TT coupling depends on the overlaps of the two highest occupied molecular orbitals (HOMOs) and two lowest unoccupied molecular orbitals (LUMOs) of the two interacting fragments; while for ET, the coupling is roughly the Fock matrix element between two HOMOs [for hole transfer (HT)] or LUMOs (for ET).[35] Therefore, the exponential distance dependence is an important characteristic of the TT coupling. For our results, the slope of the distance dependence of the coupling was fitted to be 2.82 $Å^{-1}$ (DZP basis) or 2.59 $Å^{-1}$ (6-311+G* basis) for couplings with d=3.5–6.5 Å. ET of the same two-ethylene system gives an exponent of 1.20 $Å^{-1}$ (DZP) for ET and 1.44 $Å^{-1}$ (DZP) or 1.23 $Å^{-1}$(6-311+G*) for HT.[41] The exponent of TT coupling is slightly more than the sum of the exponents derived from the ET and HT couplings. This result is similar to those reported previously. With saturated hydrocarbon spaced electron donors and acceptors, a slope of 2.6 per σ bond was reported for the TT energy-transfer rates,[20] while for ET it was 1.15 per σ bond. TT energy-transfer rates in phenylene oligomer-spaced Ru and Os dinuclear metal complexes were reported to attenuate exponentially by 0.32, 0.44, and 0.50 $Å^{-1}$.[2,3] Optically induced intervalence ET couplings between phenylene oligomer-spaced Ru complexes decay exponentially with coefficients of 0.084 or 0.118 $Å^{-1}$.[22] Multiplying the latter values by a factor of 2 to convert to the ET rates, we can see that the decay coefficients for the ET rates are roughly half of those for the TT energy transfer.

B. Couplings derived from CIS

In Fig. 4, half of the CIS energy gaps between the two lowest triplet states of two ethylenes are presented. In all cases, the two lowest triplet states are mainly composed of configurations where electrons are excited from the two highest occupied MOs to the two lowest unoccupied MOs. These resulst are very close to those from the DC scheme (deviations are smaller than 5%: see Table I). This result confirms the two-state approximation employed in Sec. II and shows that both DC and CIS can properly describe TT coupling.

In Fig. 4, we have included the results using 6-311+G* and aug-cc-pVTZ, two different basis sets that include diffusive functions. These calculations were performed as a test to see whether the long-range exponential decay is an artificial result that depends on the basis function used. The diffusive functions for carbon atoms in the 6-311+G* set are s and p type functions, both with a Gaussian exponent of 0.0438,[42] while those in the aug-cc-pVTZ set are an s function with an exponent of 0.044 02, and a set of p functions with an exponent of 0.035 69.[43] As shown in Fig. 4, the different Gaussian exponents did not change the magnitude nor the slope of the exponential decay of TT coupling. Therefore, we conclude that the couplings obtained are not artifacts of the basis functions.

C. Moving along the reaction coordinate

The energy-gap-based method relies on a resonance between the zero-order states to obtain the coupling. For asymmetric systems, this condition is not automatically fulfilled. In calculating ET couplings, an external electric field is often used to achieve the resonance condition. When scanning over the field strength, the minimal energy gap gives twice

TABLE I. TT energy transfer coupling (in meV) for a pair of ethylenes [Fig. 2(A)] calculated by direct coupling (DC) or configuration-interaction singles (CIS).

Basis set	6−31G*		DZP		6−311+G*	
Distance (Å)	DC	CIS	DC	CIS	DC	CIS
3.5	85.9	82.7	96.5	92.3	99.1	94.2
4.0	20.6	20.1	26.9	26.0	28.5	27.6
4.5	4.03	3.95	7.44	7.23	8.15	7.97
5.0	0.590	0.581	2.01	1.97	2.28	2.24

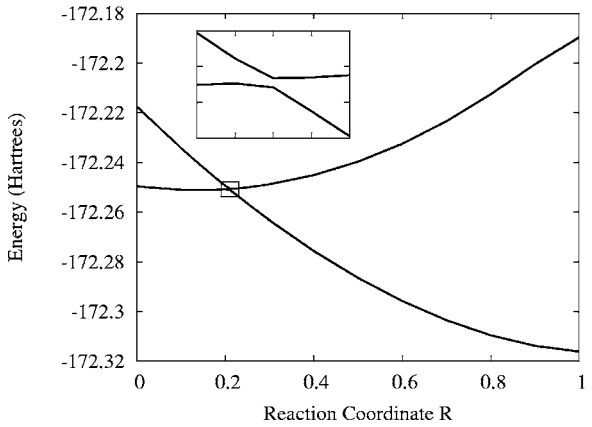

FIG. 5. Potential-energy curves of the two lowest triplet states for the ethylene-methaniminium cation system [as in Fig. 2(B)]. The reaction coordinate is as described in Eq. (25). Calculations were performed at CIS/6-31G* level, with an intermolecular distance fixed at 4.5 Å. The inset is a magnified plot of the region near the curve crossing, with grids representing 0.01 (abscissa) and 0.002 hartrees (ordinate).

the coupling value. For TT coupling, we propose varying the geometry along the reaction coordinate to control the spin localization. In Fig. 5 we report the potential-energy curves of the two lowest triplet states of an asymmetric system which is composed of a pair of isoelectronic fragments, an ethylene and a methaniminium cation, as depicted in Fig. 2(B).[44]

To find the minimum-energy gap in the ethylene-methaniminium ion, we have calculated the energies of the two lowest triplet states along the reaction coordinate. Both the CIS and DC results are included in Fig. 6. It is seen that, at separations of 3.5–5.0 Å, the CIS data closely follow the DC couplings, but are reduced by 15%–30%. Compared to the results in Table I, the discrepancy between the CIS and DC data was larger but still within the same order of magnitude. In this case, CIS and DC yielded different potential-energy curves for the two states, leading to different positions (R values) for the transition state. Such an inconsistency may increase the discrepancy in coupling, as observed in Fig. 6.

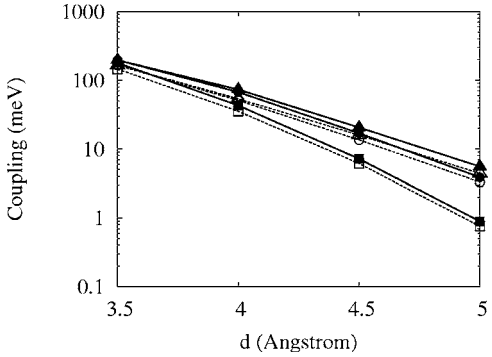

FIG. 6. TT energy-transfer coupling for the asymmetric ethylene-methaniminium ion system, face to face stacked, as shown in Fig. 2(B). The coupling calculated by HF-CIS (open symbols with dashed lines) and DC (closed symbols and solid lines) with 6-31G* (squares), DZP (circles), and 6-311+G* (triangles) basis sets. DC results were obtained at the transition-state geometry, i.e., where the minimum CIS energy gap was found.

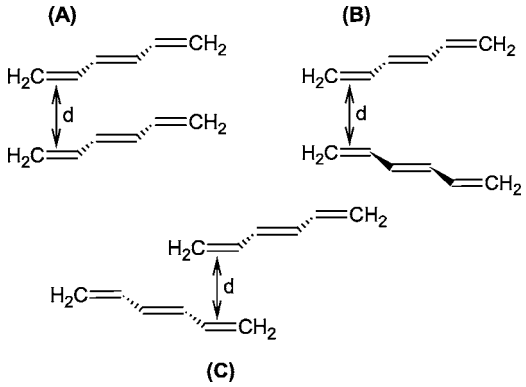

FIG. 7. Stacked pairs of hexatrienes in three different arrangements. (A) A maximum π-π contact is allowed. Panels (B) and (C) show two configurations where the close-contact area exists only in the terminal C=C π bonds. Pairs of *all-trans* butadienes and octatetraenes in similar arrangements were also studied.

D. Effects of size and intermolecular contacts

The TT coupling strengths decay steeply with increasing separation. Therefore, we expect them to depend strongly on the intermolecular contacts, since only the interactions of the nearest portions of orbitals contribute. We tested to see how the TT coupling magnitudes vary with molecular size and contact area. TT coupling between two *all-trans* polyenes was calculated for three different conformations, as depicted in Fig. 7. In one conformation (A), maximum contact between the planar molecules was created by having them fully stacked, while in the other two conformations [(B) and (C)], only the terminal C=C double bonds of the molecule were placed on top of each other.

In Fig. 8(A), we show the TT coupling of two polyenes derived from the CIS energy gaps with a large basis set (6-311+G*) over a range of separations. For the fully stacked configuration, the coupling strengths from different molecules are very similar, irrespective of their sizes. The results for partial contact are shifted towards smaller values. The ratios of the coupling strengths from the two configurations vary. For butadiene, for example, the TT coupling from the fully stacked conformation is about 2.8–3.0 times that of the partially stacked one. The extent of this reduction varies as the configuration changes. In Fig. 8(B), we see that, while keeping one pair of C=C bonds stacked, but changing the overall configuration [as depicted in Fig. 7(C)], the coupling magnitudes are further reduced, and the exponential distance dependence becomes steeper.

The weak dependence on molecular size in the full-stacked configurations can be shown to result from molecular-orbital normalization. In a simplified representation, the HOMO and LUMO of polyene oligomers are approximated as normalized linear combinations of the π and π^* of every ethylenelike unit, which are

$$\phi^* \approx \frac{1}{\sqrt{2n}} \sum_i^n (-1)^{i-1} \pi_i^*, \tag{26}$$

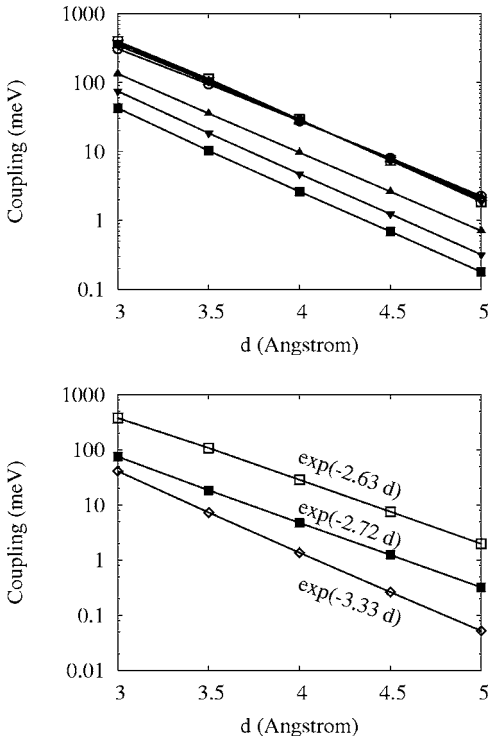

FIG. 8. Dependence of molecular size and intermolecular contacts for TT couplings. (A) Couplings are for a pair of butadienes (triangles), hexatrienes (inverse triangles), and octatetraenes (squares) at a number of intermolecular distances. The open symbols are for the results from a fully stacked configuration [Fig. 7(A)] and the closed symbols represent the results from the flipped configuration [Fig. 7(B)]. Data for a pair of ethylenes (open circles) were also included for comparison. (B) For a pair of hexatrienes, we show the coupling of fully stacked (open squares), partially stacked as in Fig. 7(B) (filled squares), and as in Fig. 7(C) (open diamonds) configurations. All the results are from CIS/6-311+G* calculations.

$$\bar{\phi} \approx \frac{1}{\sqrt{2n}} \sum_{i}^{n} (-1)^{i-1} \bar{\pi}_i, \tag{27}$$

where n is the number of double-bond units in the molecule. π_i and π_i^* are the π and π^* orbitals of the ith ethylenelike unit. Thus, the overlap integrals between two HOMOs or LUMOs are

$$\langle \bar{\phi}_D | \bar{\phi}_A \rangle = \frac{1}{2n} \left(\sum_{i}^{n} \langle \bar{\pi}_{D,i} | \bar{\pi}_{A,i} \rangle + \sum_{i \neq j}^{n} (-1)^{i+j} \langle \bar{\pi}_{D,i} | \bar{\pi}_{A,j} \rangle \right), \tag{28}$$

$$\langle \phi_D^* | \phi_A^* \rangle = \frac{1}{2n} \left(\sum_{i}^{n} \langle \pi_{D,i}^* | \pi_{A,i}^* \rangle + \sum_{i \neq j}^{n} (-1)^{i+j} \langle \pi_{D,i}^* | \pi_{A,j}^* \rangle \right), \tag{29}$$

where $\langle \phi_i | \phi_j \rangle$ denotes the inner product, or the overlap integration over spin and spacial coordinates for $\phi_i(\mathbf{x})$ and $\phi_j(\mathbf{x})$. The factor $1/2n$ outside the parentheses is the normalization factor. The first summation in the parentheses is the overlap arising from the directly stacked π-π overlaps, while the other term is the sum of all nondirectly stacked π-π overlap integrals.

Using a small STO-3G basis, we estimated the contributions of the leading terms. At a distance of 3.5 Å, the overlap integral for directly stacked π bonding orbitals is 0.385, and for π^* antibonding orbitals, it is 0.148. The overlap integral values for a $\pi(\pi^*)$ orbital to the next neighboring $\pi(\pi^*)$ orbital drop by a large factor, to 0.007 56 (π) and 0.003 63 (π^* orbitals). Therefore, the contributions of nondirectly stacked π orbitals are almost negligible in the overlap integrals. The overlap integrals as shown in Eqs. (28) and (29) essentially become independent of n, the size of the molecule. The TT coupling, which is essentially a Coulomb interaction between two overlap densities [Eq. (10)], is therefore weakly dependent on molecular size, as seen in Fig. 8(A).

In a partially contacted configuration as in Fig. 7(B), when the contact area remains the same (a pair of carbon atoms stacked), the coupling strengths become smaller with larger molecules [Fig. 8(A)]. This result indicates that the *relative* fraction of the contacting region compared to the delocalized molecular orbital is a determining factor for TT coupling.

In Fig. 8(B), it is shown that the distance attenuation factor becomes larger when there is only a partial contact between the molecules. This result, in part, reflects the complexity of the intermolecular coupling. With weakly interacting molecules, there exists an inductive effect, where the asymptotic decay of molecular orbitals is affected by the geometrical arrangements. The asymptotic potential is reduced by the presence of another molecule, leading to a slower decay in the orbital than in a vacuum. Therefore, when the two molecules are only partially stacked, with the nonstacked parts of the molecule isolated in space, the coupling extension over the space is reduced. From Figs. 8(A) and 8(B) we conclude that both the TT coupling strength and exponential decay slope depend strongly on the intermolecular configurations.

Another determining factor is the orientation of molecular contacts. Since the characteristic length of H-like orbitals does not vary with the orientation, one may expect that the distance dependence is weakly influenced by different orientations. However, for anisotropic molecules, this property will no longer hold, as is seen in the results of our tests on a pair of side-by-side ethylenes (Fig. 9). Again, with two different diffusive basis sets (6-311+G** and DZ+**), we find that the results are not dependent on the different diffusive Gaussian exponents.

Optimal overlap gives a coupling strength of ~100 meV at a distance of 3.5 Å, which can serve as an upper bound in estimating TT coupling for π-conjugated molecules. Using the golden rule rate expression, assuming that the overlap of density of states of the reactants and products is of the order of 0.1 eV^{-1}, and using a coupling strength of 100 meV, gives a TT exchange lifetime of 0.1 ps. A nanosecond TT energy-transfer lifetime corresponds to a coupling of about 1 meV, which is roughly the coupling arising from 1/4 of intermolecular contact as in the nonstacked configuration of octatetraenes at a distance of 4.5 Å.

E. Nature of TT couplings

We have reported TT energy-transfer coupling strengths with two different Hartree-Fock-based approaches. TT cou-

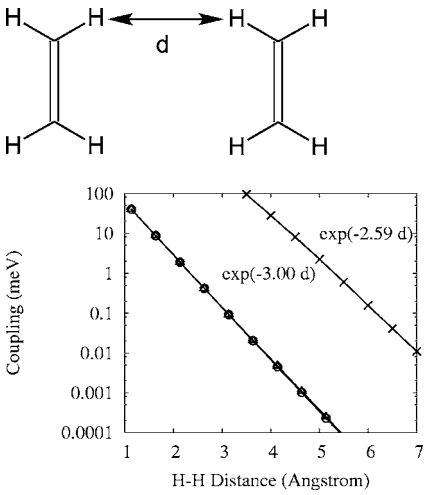

FIG. 9. Effects of orientations in TT couplings. Couplings are for a pair of side-by-side ethylenes intermolecular distances obtained by CIS/DZ+** (circles) and 6-311+G** (triangles). For comparison, the CIS/6-311+G* results for face-to-face ethylenes are included (crosses).

pling mainly arises from an exchange integral, with a steep distance dependence. We showed that the DC scheme, which has been mainly used for the ET coupling, can also be used to calculate the TT coupling if spin-localized UHF solutions are used. The calculated values from two distinct methods, the DC method and the CIS energy-gap method, agree well for both symmetric and asymmetric test systems, indicating the intrinsic consistency of the two methods.

Compared with previous calculations,[28,29] our *ab initio* TT couplings are larger by at least two orders of magnitude. The previous work was based on the PPP Hamiltonian, which ignores terms arising from the exchange integral in Eq. (10). Therefore, it is impossible to calculate the exchange interaction directly from the Hamiltonian. Instead, in Refs. 28 and 29, the authors directly integrated the necessary terms, assuming certain linear combination of Gaussian or Slater-type orbitals. In Ref. 29, the influence of superexchange through other atoms was also included. It is not clear to us what the exact source of the large discrepancy between our *ab initio* results and the previous semiempirical calculations is, and below we discuss more possibilities.

For ET couplings, calculations using semiempirical Hamiltonians typically yield values similar to those of *ab initio* models.[45,46] Recently, Chen and Hsu found that *ab initio* ET couplings are larger by a factor of 3 and decay more slowly than those from a semiempirical Hamiltonian.[47] Using H-like orbitals, Levy and Speiser's data[26] found an exponent for the exchange integral to be about 4.5 $Å^{-1}$, as inferred from Fig. 6 of Ref. 26, a much larger value than we found. In Ref. 29, the smallest exponent used for the $2p\pi$ atomic orbitals was 1.054 $bohrs^{-1}$, leading to a steep exponential distance attenuation (about 4 $Å^{-1}$ for exchange integrals). The differences in attenuation rates may in part account for the large discrepancy between our results and previous calculations. The weaker distance dependence we observe may also arise from the change of the asymptotic potential due to the presence of another molecule. All atoms or molecules have positive electron affinities, and therefore the asymptotic potential is lower than in a vacuum. As a result, an electron is likely to extend to a larger distance when it is mediated by an atom or a molecule. With semiempirical Hamiltonians, the interactions among orbitals are limited by the parametrization, which may fall off steeply with distance since the presence of a neighboring molecule is not considered. Such an effect may be more significant for TT coupling than for ET, since the exchange integral is composed of four molecular orbitals, while only two molecular orbitals are involved in the major term of ET coupling,.

The results from varying molecular sizes and contact area indicate that the TT coupling is mainly determined by the relative contact area, with respect to the size of molecular orbitals. When the polyene molecules were 100% stacked, the coupling strengths and attenuation rates were very similar irrespective of their sizes. On the other hand, when there was only a fraction of the molecules in close contact, the coupling strengths dropped by large factor. The two different partially stacked configurations exhibited different exponents for the coupling, and both were larger than that of the fully stacked molecules. A pair of H–H (side-by-side) contacting ethylenes also gave rise to a steeper distance dependence. This indicates that the the rate of exponential attenuation depends on how the molecules are stacked and on the orientation of the interacting π orbitals.

With hydrogen-like orbitals, the distance dependence of exchange rate can be estimated to follow $\exp(-2R/L)$, where L is the average orbital radius involved in the electron exchange.[26] In much of the experimental literature, L has been replaced by the van der Waals or Bohr radii for estimating the Dexter coupling (e.g., Refs. 18 and 19). For example, for porphyrins, $L=4.8$ Å was used as a guide to interpret the experimental results,[18] which led to an attenuation rate of 0.416 $Å^{-1}$, much smaller than our calculated value, 2.6 $Å^{-1}$. The most serious problem in using this rough estimate is that it is very difficult to properly estimate L. The assumption of hydrogenlike orbitals is only valid for transitions to Rydberg states. For valence triplet states, L is probably close to the characteristic radius of a carbon p orbital, since the π and π^* orbitals involved are mainly composed of these atomic orbitals, instead of the size of the full molecule. This is also illustrated in Fig. 8(A), where the exponential decay slopes are very similar, irrespective of their sizes.

For the singlet-singlet energy transfer, we would like to stress that a deviation from R^{-6} dependence at short distance does not rule out the Coulomb contribution to the coupling. We showed that a reasonable upper bound for exchange coupling is about 100 meV, obtained at 3.5 Å, with a full π-π contact. The Coulomb couplings can be at least this large at short distances. When separated by short distances, the singlet-singlet energy-transfer couplings may be a mixture of Coulomb and exchange elements, both with distance dependence that is steeper than the typical dipole-dipole R^{-6}.

F. TT energy-transfer rates

TT energy transfer between Chls and Cars is of great importance in the photoprotection of plants and photosynthetic bacteria. With previously calculated values it was dif-

ficult to understand the difference in magnitudes of the observed rates and the theoretically calculated ones. In this section we briefly explore whether our calculated coupling is adequate to explain the experimental data.

The recently published crystal structure of the major light-harvesting complex II (LHCII) of green plants shows many close contacts between Chls and Cars.[48–50] The LHCII crystal was further shown to be in a dissipative state where chlorophyll fluorescence is quenched.[50] In the crystal structure, the two luteins are at a distance of 3.6 Å from two Chl *a* molecules.[49] The π-π contact is about $1/2-1/3$ of the full π delocalization area in the two pairs of molecules. From our results described above, we can roughly estimate the TT coupling between the lutein and Chl *a* to be of the order of 10 meV. The actual TT transfer rate depends on the degree of overlap in the density of states, but the coupling in this range suggests the TT energy transfer could be in the picosecond range.

The triplet state kinetics of Car and Bchl *a* phosphorescence in the LH2 antenna complex from purple bacteria was measured recently.[8] The decay times of the triplet states of Car and Bchl are 2.0 and 1.8 ns, respectively. A triplet-triplet annihilation reaction was proposed. In this mechanism, both triplet states Bchl and Car simultaneously annihilate, and Q_y singlet Bchl is generated. TT annihilation is similar to TT energy-transfer, which also involves the exchange of two electrons of different spin and energy. An electronic coupling of 10 meV could easily lead to the observed nanosecond lifetimes of the triplet state species.

IV. CONCLUSIONS

We have developed two different approaches to calculate TT energy-transfer couplings between a pair of molecules. For both asymmetric and symmetric test systems, the direct coupling method and the energy-gap-based CIS scheme yielded very similar results. Tests using basis sets with different diffusive functions yielded essentially the same results, indicating that the values we obtained are consistent within the Hartree-Fock theoretical framework. With a series of fully stacked polyene oligomer pairs, we found that the TT coupling strengths and attenuation rates are very similar, irrespective of the size of the π-conjugated molecules. For partially stacked configurations, the coupling magnitudes are reduced as the relative sizes of the contact regions are reduced. For closely spaced molecules, the calculated TT coupling values imply picosecond or nanosecond TT exchange time scales.

ACKNOWLEDGMENTS

Two of the authors (C.P.H. and Z.Q.Y.) acknowledge the National Science Council of Taiwan (Grant No. NSC93-2113-M-001-012). One of the authors (Z.Q.Y.) wishes to acknowledge financial support from Academia Sinica. The work at Berkeley was supported by the Director, Office of Science, Office of Basic Energy Sciences, Chemical Sciences Division, of the U.S. Department of Energy under Contract No. DE-AC03-76SF00098.

[1] R. Ziessel, M. Hissler, A. El-Ghayoury, and A. Harriman, Coord. Chem. Rev. **178**, 1251 (1998).
[2] B. Schlicke, P. Nelser, L. De Cola, E. Sabbioni, and V. Balzani, J. Am. Chem. Soc. **121**, 4207 (1999).
[3] A. D'Aéo, S. Welter, E. Cecchetto, and L. De Cola, Pure Appl. Chem. **77**, 1035 (2005).
[4] R. R. Islangulov, D. V. Kozlog, and F. N. Castellano, Chem. Commun. (Cambridge) **30**, 3776 (2005).
[5] *The Photochemistry of Carotenoids*, edited by H. A. Frank, A. J. Young, G. Nritton, and R. J. Cogdell (Kluwer, The Netherlands, 1999).
[6] N. I. Krinsky, Philos. Trans. R. Soc. London, Ser. B **284**, 581 (1978).
[7] R. J. Cogdell and H. A. Frank, Biochim. Biophys. Acta **895**, 63 (1987).
[8] F. S. Rondonuwu, T. Taguchi, R. Fujii, K. Yokoyama, Y. Koyama, and Y. Watanabe, Chem. Phys. Lett. **384**, 364 (2004).
[9] R. J. Cogdell, T. D. Howard, R. Bittl, E. Schlodder, I. Geisenheimer, and W. Lubitz, Philos. Trans. R. Soc. London, Ser. B **355**, 1345 (2000).
[10] C. S. Foote and R. W. Denny, J. Am. Chem. Soc. **90**, 6233 (1968).
[11] D. L. Dexter, J. Chem. Phys. **21**, 836 (1953).
[12] T. Förster, Ann. Phys. (Leipzig) **2**, 55 (1948).
[13] R. McWeeny, *Methods of Molecular Quantum Mechanics*, 2nd ed. (Academic Press, London, 1992).
[14] C.-P. Hsu, G. R. Fleming, M. Head-Gordon, and T. Head-Gordon, J. Chem. Phys. **114**, 3065 (2001).
[15] G. D. Scholes, Annu. Rev. Phys. Chem. **54**, 57 (2003).
[16] B. P. Krueger, G. D. Scholes, and G. R. Fleming, J. Phys. Chem. B **102**, 5378 (1998).
[17] C.-P. Hsu, P. J. Walla, M. Head-Gordon, and G. R. Fleming, J. Phys. Chem. B **105**, 11016 (2001).
[18] S. Faure, C. Stern, R. Guilard, and P. D. Harvey, J. Am. Chem. Soc. **126**, 1253 (2004).
[19] J. A. Mondal, G. Ramakrishna, A. K. Singh, H. N. Ghosh, M. Mariappan, B. G. Maiya, T. Muskherjee, and D. K. Palit, J. Phys. Chem. A **108**, 7843 (2004).
[20] G. L. Closs, P. Piotrowiak, J. M. MacInnis, and G. R. Fleming, J. Am. Chem. Soc. **110**, 2652 (1988).
[21] G. L. Closs, M. D. Johnson, J. R. Miller, and P. Piotrowiak, J. Am. Chem. Soc. **111**, 3751 (1989).
[22] J.-P. Launay, Chem. Soc. Rev. **30**, 386 (2001).
[23] J. L. Katz, J. Jortner, S. I. Choi, and S. A. Rice, J. Chem. Phys. **39**, 1897 (1963).
[24] J. Jortner, S.-I. Choi, J. L. Katz, and S. A. Rice, Phys. Rev. Lett. **11**, 323 (1963).
[25] J. Jortner, S. A. Rice, J. L. Katz, and S. I. Choi, J. Chem. Phys. **42**, 309 (1964).
[26] S.-T. Levy and S. Speiser, J. Chem. Phys. **96**, 3585 (1992).
[27] N. Koga, K. Sameshima, and K. Morokuma, J. Phys. Chem. **97**, 13117 (1993).
[28] H. Nagae, T. Kakitani, T. Katoh, and M. Mimuro, J. Chem. Phys. **98**, 8012 (1993).
[29] A. Damjanovic, T. Ritz, and K. Schulten, Phys. Rev. E **59**, 3293 (1999).
[30] A. Aspuru-Guzik, O. E. Akramine, J. C. Grossman, and W. A. Lester, Jr., J. Chem. Phys. **120**, 3049 (2004).
[31] A. H. A. Clayton, G. D. Scholes, K. P. Ghiggino, and M. N. Paddon-Row, J. Phys. Chem. **100**, 10912 (1996).
[32] K. Ohta, G. L. Closs, K. Morokuma, and N. J. Green, J. Am. Chem. Soc. **108**, 1319 (1986).
[33] A. Broo and S. Larsson, Chem. Phys. **148**, 103 (1990).
[34] A. Farazdel, M. Dupuis, E. Clementi, and A. Aviram, J. Am. Chem. Soc. **112**, 4206 (1990).
[35] L. Y. Zhang, R. A. Friesner, and R. B. Murphy, J. Chem. Phys. **107**, 450 (1997).
[36] M. D. Newton and N. Sutin, Annu. Rev. Phys. Chem. **35**, 437 (1984).
[37] A. Szabo and N. S. Ostlund, *Modern Quantum Chemistry: Introduction to Advanced Electronic Structure Theory*, 1st ed. (McGraw-Hill, New York, 1993).
[38] J. B. Foresman, M. Head-Gordon, J. A. Pople, and M. J. Frisch, J. Phys. Chem. **96**, 135 (1992).
[39] E. Kreyszig, *Advanced Engineering Mathematics*, 8th ed. (Wiley, New York, 1999).
[40] J. Kong, C. A. White, A. I. Krylov *et al.*, J. Comput. Chem. **21**, 1532 (2000).
[41] Z.-Q. You, Y. Shao, and C.-P. Hsu, Chem. Phys. Lett. **390**, 116 (2004).
[42] T. Clark, J. Chandrasekhar, G. W. Spitznagel, and P. v. R. Schleyer, J. Comput. Chem. **4**, 294 (1983).

[43] R. A. Kendall, T. H. Dunning, Jr., and R. J. Harrison, J. Chem. Phys. **96**, 6796 (1992).
[44] M. Rust, J. Lappe, and R. J. Cave, J. Phys. Chem. A **106**, 3930 (2002).
[45] M. D. Newton, in *Cluster Models for Surface and Bulk Phenomena*, NATO Advance Studies Institute, Series B: Physics, edited by G. Pacchioni, P. S. Bagus, and F. Parmigiani (Plenum, New York, 1992), Vol. 283, p. 551.
[46] M. D. Newton, J. Phys. Chem. **92**, 3049 (1988).
[47] H.-C. Chen and C.-P. Hsu, J. Phys. Chem. A (in press).
[48] Z. Liu, H. Yan, K. Wang, T. Kuang, J. Zhang, L. Gui, X. An, and W. Chang, Nature (London) **428**, 287 (2004).
[49] J. Standfuss, A. C. T. van Scheltinga, M. Lamborghini, and W. Kühlbrandt, EMBO J. **24**, 919 (2005).
[50] A. A. Pascal, Z. Liu, K. Nroess, B. van Oort, H. van Amerongen, C. Wang, P. Horton, B. Robert, W. Chang, and A. Ruban, Nature (London) **436**, 134 (2005).